J|A|C|S COMMUNICATIONS

Published on Web 02/23/2010

Shape-Directed Assembly of a "Macromolecular Barb" into Nanofibers: Stereospecific Cyclopolymerization of Isopropylidene Diallylmalonate

Yasunao Miyamura,[†] Kazushi Kinbara,*[,†] Yohei Yamamoto,[‡] Vakayil K. Praveen,[‡] Kenichi Kato,[§] Masaki Takata,[§] Atsushi Takano,[||] Yushu Matsushita,[||] Eunji Lee,[⊥] Myongsoo Lee,[⊥] and Takuzo Aida*[,†,‡]

Department of Chemistry and Biotechnology, The University of Tokyo, 7-3-1 Hongo, Bunkyo-ku, Tokyo 113-8656, Japan, ERATO-SORST Nanospace Project, Japan Science and Technology Agency (JST), National Museum of Emerging Science and Innovation, 2-41 Aomi, Koto-ku, Tokyo 135-0064, Japan, RIKEN SPring-8 Center, 1-1-1 Kouto, Sayo-cho, Sayo-gun, Hyogo 679-5148, Japan, Department of Applied Chemistry, Nagoya University, Furo-cho, Chikusa-ku, Nagoya 464-8603, Japan, and Center for Supramolecular Nano-Assembly and Department of Chemistry, Seoul National University, 599 Kwanak-ro, Seoul 151−747, Republic of Korea

Received December 26, 2009; E-mail: kinbara@tagen.tohoku.ac.jp; aida@macro.t.u-tokyo.ac.jp

Ordered molecular assembly in solution generally requires sufficiently strong and directional forces given by, e.g., hydrogen-bonding,[1] π-electronic,[2] and/or metal-ligating interactions.[3] In contrast, van der Waals interactions are inherently weak and nondirectional and by themselves hardly induce ordered assembly if not assisted by directional forces. Peptide amphiphiles[4a] and paraffinic oligothiophenes[4b] are typical examples that self-assemble regularly into nanofibers by combining a directional interaction with a van der Waals force.[4] These nanofibers can eventually be cross-linked to cause physical gelation of solvents.[4] Here we report that a "barb"-shaped polymer self-assembles into regular nanofibers *solely* by a van der Waals interaction. This work was prompted by our serendipitous finding that a physical gel forms when isopropylidene diallylmalonate (**1**)[5] is allowed to polymerize in CH_2Cl_2 using newly designed α-diimine Pd(II) complex **3** (Figure 1a). Unprecedentedly, the produced cycloolefinic polymer (**2**) is highly rich in *threo*-disyndiotactic sequences (st_{rich}-**2**) and, on the basis of a molecular model of its stereochemically pure 16-mer, likely adopts a barb shape (Figure 1b) with its cyclic malonate pendants sticking out alternately up and down along the main chain. Polyolefins such as branched polyethylene and isotactic polypropylene are known to form physical gels. However, in these cases, the polymer molecules self-assemble not into nanofibers but into spherulites, which are responsible for the formation of a cross-linked 3D network structure essential for physical gelation.[6] Apart from polyolefins, poly(lactic acid)[7] and poly(methyl methacrylate) (PMMA)[8,9] are known as rare examples that give rise to physical gelation only by van der Waals interactions. However, in the former case, spherulites are again responsible for the formation of a 3D network.[7] Although the latter example is similar to our system in that nanofibers are formed solely by van der Waals interactions, this particular assembly occurs only when isotactic and syndiotactic PMMAs are mixed together.[8,9]

Initiator **3** features a cyclic ligand with an azobenzene strap on one side and an α-diimine unit[10] that accommodates a chloro(methyl)palladium(II) species on the other. We succeeded in crystallographic determination of the structure of as-synthesized **3** and confirmed that the azobenzene unit adopts a *trans* form (Figure 2). The crystal structure also shows that *trans*-**3** possesses C_1 symmetry, with one side of the Pd(II) center sterically blocked by the azobenzene strap. The initial purpose of the present study was to develop an initiator that is capable of photochemically switching its polymerization activity. We chose polymerization of **1**, which has been reported by Osakada et al.[5] to proceed stereospecifically

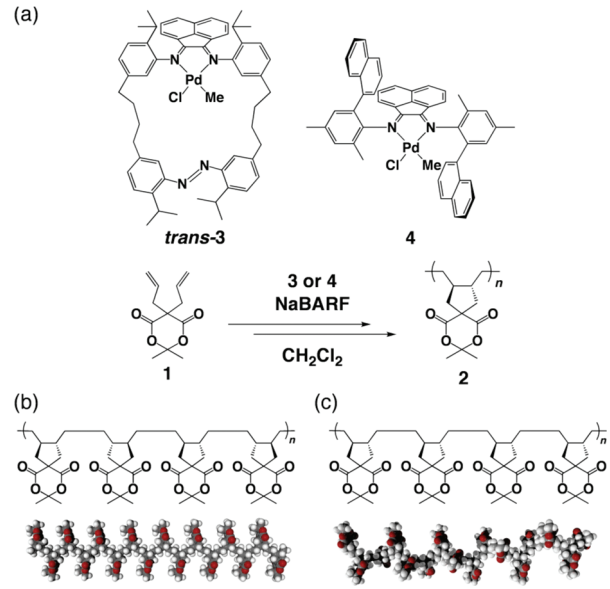

Figure 1. (a) Polymerization of diallylmalonate **1** initiated by α-diimine Pd(II) complexes **3** (this work) and **4** (ref 5). Also shown are structures and computer-generated CPK models of 16-mers of **1** composed exclusively of (b) *threo*-disyndiotactic (*st*-**2**) and (c) *threo*-diisotactic (*it*-**2**) sequences.

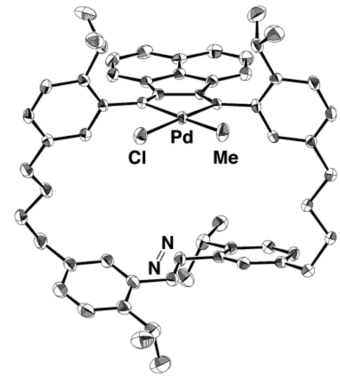

Figure 2. Crystal structure (ORTEP diagram) of *trans*-**3**, showing 50% probability thermal ellipsoids. H atoms have been omitted for clarity.

[†] The University of Tokyo.
[‡] Japan Science and Technology Agency.
[§] RIKEN SPring-8 Center.
[||] Nagoya University.
[⊥] Seoul National University.

10.1021/ja910901e

Table 1. Polymerization of **1** Initiated with α-Diimine Complexes *trans*-**3**, *cis*-**3** (80%), and **4** in CH_2Cl_2[a]

run	Initiator (Ini)	$[\mathbf{1}]_0/[\mathrm{Ini}]_0$	temp (°C)	time (h)	conv (%)	M_n	M_w/M_n	$\%S_{tetrad}$[c]
1	*trans*-**3** (10)[b]	100	25	24	100	4300	1.92	42
2	*trans*-**3** (5)[b]	200	25	60	90	4200	1.61	42
3	*trans*-**3** (10)[b]	100	0	48	44	8400	1.68	60
4	*trans*-**3** (10)[b]	100	0	120	86	8600	2.09	60
5	*trans*-**3** (20)[b]	100	−10	192	65	15800	1.65	60
6	*cis*-**3** (80%) (12)[b]	120	25	48	98	3700	2.09	n.d.
7	**4** (40)[b]	100	0	168	100	6500	1.92	n.d.

[a] $[\mathrm{NaBARF}]_0/[\mathrm{Ini}]_0 = 1.2$. [b] The value in parentheses is $[\mathrm{Ini}]_0$ (in mM). [c] Syndiotactic tetrad content (in %).

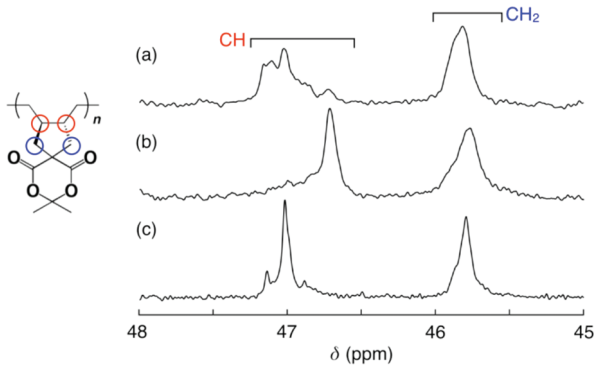

Figure 3. ^{13}C NMR spectra ($CDCl_3$, 25 °C) of (a) **2** with low stereoregularity,[12] (b) it_{rich}-**2** formed using **4**,[5] and (c) st_{rich}-**2** formed using *trans*-**3** (Table 1, run 3).

using C_2-symmetric α-diimine Pd(II) initiator **4** in conjunction with NaBARF,[11] affording polymer **2** that is rich in *threo*-diisotactic sequences (it_{rich}-**2**).[5] When **1** was allowed to polymerize with *trans*-**3** in CH_2Cl_2 at 25 °C ($[\mathbf{1}]_0/[\mathbf{3}]_0/[\mathrm{NaBARF}]_0 = 100/1/1.2$), the polymerization system entirely underwent gelation within 12 h. After 24 h, **1** was consumed completely, affording **2** with M_n and M_w/M_n of 4300 and 1.92, respectively, as estimated using polystyrene standards (Table 1, run 1). For evaluating the activity of *cis*-**3**, we used a 20/80 mixture of *trans*-**3** and *cis*-**3**, since pure *cis*-**3** was unavailable photochemically.[12] The polymerization of **1** with this mixed initiator system took place sluggishly, reaching quantitative monomer conversion in 48 h (Table 1, run 6). With the assumption of pseudo-first-order kinetics, the activity of *cis*-**3** for the polymerization of **1** was estimated as only $^1/_{20}$ that of *trans*-**3**.[12] Thus, the geometry of the azobenzene strap significantly affects the polymerization activity of **3**.

Analogous to reported α-diimine Pd(II) initiators,[5] *trans*-**3** and 20/80 *trans*-**3**/*cis*-**3** allowed for complete cyclization of the two allylic groups of **1** to afford, in the polymer main chain, *trans*-1,2-disubstituted cyclopentane units (**2**) whose relative configurations give rise to tacticity. Accordingly, in ^{13}C NMR spectroscopy, polymer **2** could in principle show eight singlet CH signals corresponding to eight possible tetrads.[5,12] Of particular interest, **2** obtained with *trans*-**3** (Table 1, run 1) showed a highly enhanced CH signal at 47.0 ppm. Such an enhancement was more explicit when the polymerization was conducted at lower temperatures, such as 0 °C (Table 1, run 3; Figure 3c) and −10 °C (Table 1, run 5). Among the eight possible tetrads,[12] only the diisotactic or disyndiotactic tetrad content can be enhanced when the polymerization proceeds stereospecifically. With reported initiator **4**,[5] it_{rich}-**2** was prepared as a reference (Table 1, run 7), which allowed us to confirm a marked enhancement of the CH signal at 46.7 ppm (Figure 3b). Hence, the intense CH signal at 47.0 ppm for polymer **2** obtained with *trans*-**3** (Figure 3c) can be assigned to the *threo*-disyndiotactic sequence.[13] On the basis of a fitted spectrum using Lorentz functions,[12] the *threo*-disyndiotactic diad, triad, and tetrad contents in the polymer chain were evaluated as 84, 71, and 60%, respectively (Table 1, run 3).[12]

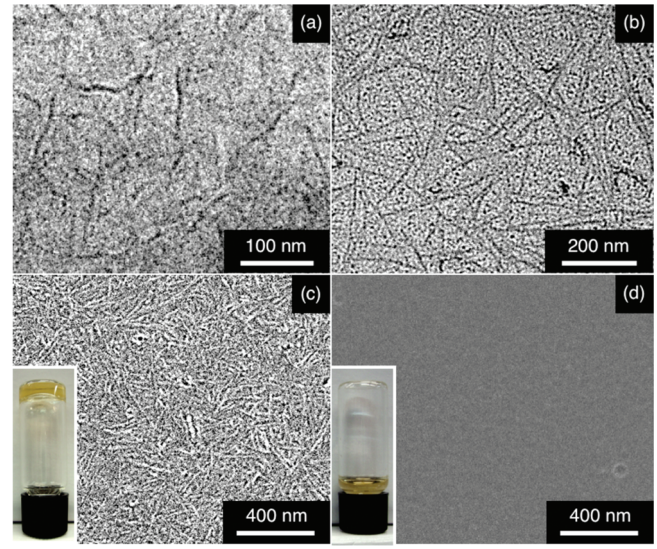

Figure 4. (a) Cryogenic TEM micrograph of a $Cl_2CHCHCl_2$ solution of st_{rich}-**2**. (b) TEM and (c) SEM micrographs of an air-dried sample prepared from a CH_2Cl_2 solution of st_{rich}-**2**. (d) SEM micrograph of an air-dried sample prepared from a CH_2Cl_2 solution of it_{rich}-**2** as a reference. Insets: pictures of (c) st_{rich}-**2** and (d) it_{rich}-**2** in CH_2Cl_2 (14 wt %) after heating followed by cooling.

Size-exclusion chromatography using a refractive index/UV−vis dual detector suggested that st_{rich}-**2** as-synthesized using *trans*-**3** carried at its active end an initiator fragment, which was successfully cleaved off using Et_3SiH.[12] We confirmed that the resultant polymer bearing no initiator fragment can also induce gelation of halogenated solvents such as CH_2Cl_2 upon heating followed by cooling (Figure 4c inset and Table S2 in the SI).[12] Using a smaller amount of st_{rich}-**2** for the heating/cooling treatment in CH_2Cl_2 resulted in the formation of a weak gel. When this weak gel was subjected to centrifugation, a liquid phase clearly separated from a gel phase, indicating a critical gelation concentration (CGC). As the polymer molecular weight increased ($M_n = 4200 \rightarrow 8400 \rightarrow 15800$), the CGC decreased (22 → 14 → 10 wt %). In contrast, no gelation of CH_2Cl_2 occurred when it_{rich}-**2** prepared using initiator **4**[5] (Table 1, run 7) was used in place of st_{rich}-**2** (Figure 4d, inset). Thus, the tacticity of polymer **2** plays a critical role in the gelation of CH_2Cl_2.

The physical gelation of CH_2Cl_2 indicates that st_{rich}-**2** self-assembles to form a 3D network structure. As shown in Figure 4b,c, nanofibers with an average diameter of ∼10 nm were visualized by transmission electron microscopy (TEM) and scanning electron microscopy (SEM) of an air-dried sample of st_{rich}-**2** (Table 1, run 4) prepared from its CH_2Cl_2 solution. Nanofiber formation also occurred with lower-molecular-weight st_{rich}-**2** (Table 1, run 2).[12] By means of cryogenic TEM, we confirmed that such nanofibers form even in dilute solution (Figure 4a). Consistently, dynamic light-scattering (DLS) analysis at 20 °C (Figure 5a) of a 2 wt % CH_2Cl_2 solution of st_{rich}-**2** (dashed curve) showed the presence of light-scattering species whose hydrodynamic diameters increased as the concentration of st_{rich}-**2** increased (8 wt %; solid curve). Its solution viscosity was highly sensitive to the concentration of st_{rich}-**2** (Figure 5b, blue) even when it was lower than the CGC. In sharp contrast, as shown in Figure 4d, no nanofibers were observed for it_{rich}-**2** (Table 1, run 7). Its CH_2Cl_2 solution (8 wt %) was virtually DLS-silent. Furthermore, the viscosity remained almost constant as the concentration of it_{rich}-**2** increased from 0 to 2 wt % (Figure

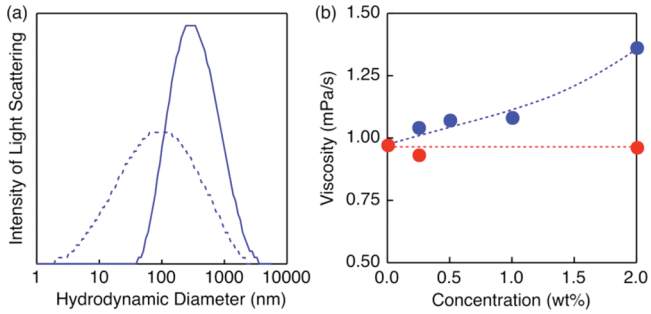

Figure 5. (a) DLS profiles at 20 °C for CH_2Cl_2 solutions of st_{rich}-**2** (Table 1, run 4) at concentrations of 2 (dashed curve) and 8 wt % (solid curve). (b) Viscosities of CH_2Cl_2 solutions of st_{rich}-**2** (Table 1, run 4) (blue) and it_{rich}-**2** (Table 1, run 7) (red) at different concentrations.

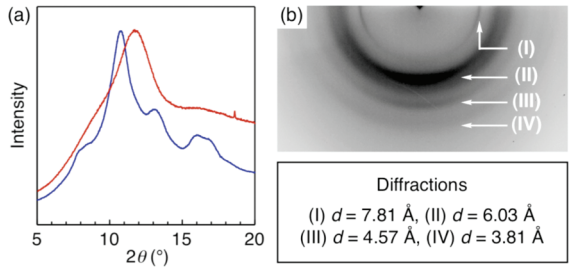

Figure 6. (a) XRD patterns of powder samples of st_{rich}-**2** (blue) and it_{rich}-**2** (red) as a reference, prepared with *trans*-**3** and **4**[5] as initiators, respectively. (b) WAXD pattern of a film sample (nanofibers) of st_{rich}-**2** (edge view).

5b, red). The contrasting self-assembling behaviors thus observed for st_{rich}-**2** and it_{rich}-**2** are quite interesting, since only van der Waals forces, which are inherently nondirectional, are operative for the self-assembly of **2**. As shown in Figure 1, molecular models predict that stereochemically pure *it*-**2** likely adopts a helical geometry (panel c), while *st*-**2** adopts a barb shape (panel b). We also noticed that the rigid cyclic malonate pendants of *st*-**2** play a critical role in its unique assembling behavior, since a derivative of st_{rich}-**2** bearing "acyclic" malonate pendants (methyl ester) did not assemble into nanofibers under identical conditions.[12]

A powder sample prepared from a CH_2Cl_2 solution of it_{rich}-**2** was amorphous and did not show any crystalline features in its X-ray diffraction (XRD) profile (Figure 6a, red). In sharp contrast, powder XRD analysis of st_{rich}-**2** displayed several diffraction peaks (blue). When the thin film of the nanofibers of st_{rich}-**2** used for SEM microscopy (Figure 4c) was subjected to wide-angle X-ray diffraction (WAXD) analysis, its edge view displayed an anisotropic pattern with four distinct diffractions (Figure 6b), three of which (II−IV) were enhanced in the meridian region while the fourth (I) was enhanced in the equator region. Since the majority of the nanofibers lie in an orientation planar to the film (Figure 4c), this anisotropic diffraction pattern is reasonable. As the initial step for the nanofiber formation, we propose that the polymer self-assembles bilaterally into 2D tapes, which further self-assemble in a face-to-face fashion into nanofibers (Figure S13 in the SI).[12] If the bilateral assembly of *st*-**2** is triggered by interdigitation of its cyclic malonate pendants, the distances for the main chains and malonate pendants estimated from the molecular model of *st*-**2** (Figure 1b) would be 11.2 and 9.2 Å, respectively. On the other hand, the face-to-face-assembled 2D tapes are estimated to be separated by 7.4 Å. The observed WAXD pattern is consistent with an orthogonal lattice whose lattice parameters *a*, *b* (meridian diffractions II−IV), and *c* (equator diffraction I) of 12.1, 9.1, and 7.8 Å, respectively,[12] can be rationalized by the proposed packing model (Figure S13). It should be noted that bilateral self-assembly via side-chain interdigitation has never been reported for polymers with rigid side chains on a rigid backbone.[14]

Prompted by unexpected physical gelation of solvents, we noticed that cyclic α-diimine Pd(II) complex *trans*-**3** is the first initiator to cause syndiospecific cyclopolymerization of isopropylidene diallylmalonate (**1**),[5] affording a barb-shaped polymer (Figure 1b). In halogenated solvents, this polymer, in contrast to its isotactic reference, self-assembles into nanofibers, eventually leading to the formation of a 3D network structure essential for physical gelation. This is in sharp contrast to known polymer physical gels, where polymer molecules assemble into spherulites rather than fibers for cross-linking.[6,7] Further studies are in progress to elucidate the origin of the syndiospecificity of *trans*-**3** and tailor barb-shaped *st*-**2** to develop particular functions.

Acknowledgment. We thank Dr. M. Yamashita for supporting X-ray crystallography, Profs. K. Osakada and D. Takeuchi for generous discussions, and Prof. M. Shimomura, Dr. H. Yabu, and Mr. M. Ara for viscosity measurements. The synchrotron radiation experiments were performed at BL44B2 at SPring-8 with the approval of RIKEN (Proposal 20090021). This work was partially supported by the Ministry of Education, Culture, Sports, Science and Technology, Japan, Grants-in-Aid for Scientific Research on Innovative Areas to K.K. (Photochromism 471) and T.A. (Emergence in Chemistry 2010).

Supporting Information Available: Synthesis of **3**, X-ray crystallographic data for *trans*-**3** (CIF), polymerization of **1**, SEM and TEM micrographs of **2** and a derivative, DLS profiles of CH_2Cl_2 solutions of **2**, DSC and TGA profiles of **2**, and the WAXD profile of st_{rich}-**2**. This material is available free of charge via the Internet at http://pubs.acs.org.

References

(1) (a) Lehn, J.-M. *Supramolecular Chemistry*; VCH: Weinheim, Germany, 1995. (b) Brunsveld, L.; Folmer, B. J. B.; Meijer, E. W.; Sijbesma, R. P. *Chem. Rev.* **2001**, *101*, 4071. (c) Palmer, L. C.; Stupp, S. I. *Acc. Chem. Res.* **2008**, *41*, 1674.
(2) (a) Percec, V.; Dimitris, T. *Contemp. Top. Polym. Sci.* **1992**, *7*, 247. (b) Lee, M.; Cho, B.; Zin, W. *Chem. Rev.* **2001**, *101*, 3869. (c) Hoeben, F. J. M.; Jonkheijm, P.; Meijer, E. W.; Schenning, A. P. H. J. *Chem. Rev.* **2005**, *105*, 1491. (d) Aida, T.; Fukushima, T. *Phil. Trans. R. Soc. London, Ser. A* **2007**, *365*, 1539.
(3) (a) Fujita, M. *Chem. Soc. Rev.* **1998**, *27*, 417. (b) Eddaoudi, M.; Moler, D. B.; Li, H.; Chen, B.; Reineke, T. M.; O'Keeffe, M.; Yaghi, O. M. *Acc. Chem. Res.* **2001**, *34*, 319.
(4) (a) Hartgerink, J. D.; Beniash, E.; Stupp, S. I. *Science* **2001**, *294*, 1684. (b) Henze, O.; Feast, W. J.; Gardebien, F.; Jonkheijm, P.; Lazzaroni, R.; Lèclere, P.; Meijer, E. W.; Schenning, A. P. H. J. *J. Am. Chem. Soc.* **2006**, *128*, 5923. (c) Jonkheijm, P.; van der Schoot, P.; Schenning, A. P. H. J.; Meijer, E. W. *Science* **2006**, *313*, 80. (d) Moon, K.-S.; Kim, H.-J.; Lee, E.; Lee, M. *Angew. Chem., Int. Ed.* **2007**, *46*, 6807.
(5) (a) Park, S.; Takeuchi, D.; Osakada, K. *J. Am. Chem. Soc.* **2006**, *128*, 3510. (b) Okada, T.; Park, S.; Takeuchi, D.; Osakada, K. *Angew. Chem., Int. Ed.* **2007**, *46*, 6141.
(6) Recent examples of polyolefin gels: (a) Matsuda, H.; Inoue, T.; Okabe, M.; Ukaji, T. *Polym. J.* **1987**, *19*, 323. (b) Matsuda, H.; Kashiwagi, R.; Okabe, M. *Polym. J.* **1988**, *20*, 189.
(7) Recent examples of poly(lactic acid) stereocomplex gels: (a) Tsuji, H.; Ikada, Y. *Polymer* **1999**, *40*, 6699. (b) Tsuji, H. *Macromol. Biosci.* **2005**, *5*, 569.
(8) (a) Schomaker, E.; Challa, G. *Macromolecules* **1989**, *22*, 3337. (b) Kumaki, J.; Kawauchi, T.; Okoshi, K.; Kusanagi, H.; Yashima, E. *Angew. Chem., Int. Ed.* **2007**, *46*, 5348. (c) Kumaki, J.; Kawauchi, T.; Ute, K.; Kitayama, T.; Yashima, E. *J. Am. Chem. Soc.* **2008**, *130*, 6373.
(9) Recent examples of PMMA gels: (a) Quintana, J. R.; Stubbersfield, R. B.; Price, C.; Katime, I. A. *Eur. Polym. J.* **1989**, *25*, 973. (b) Quintana, J. R.; Stubersfield, R.; Price, C.; Katime, I. *J. Polym. Sci., Part B: Polym. Phys.* **1990**, *28*, 1565.
(10) Selected examples of Ni(II) and Pd(II) α-diimine initiators: (a) Ittel, S. D.; Johnson, L. K.; Brookhart, M. *Chem. Rev.* **2000**, *100*, 1169. (b) Cherian, A. E.; Rose, J. M.; Lobkovsky, E. B.; Coates, G. W. *J. Am. Chem. Soc.* **2005**, *127*, 13770. (c) Leung, D. H.; Ziller, J. W.; Guan, Z. *J. Am. Chem. Soc.* **2008**, *130*, 7538.
(11) NaBARF = Sodium tetrakis[3,5-bis(trifluoromethyl)phenyl]borate.
(12) See the Supporting Information (SI).
(13) For discussion of the origin of syndiospecificity, see pp S17−S18 in the SI.
(14) (a) Inomata, K.; Nakanishi, E.; Sakane, Y.; Koike, M.; Nose, T. *J. Polym. Sci., Part B: Polym. Phys.* **2005**, *43*, 79. (b) Inomata, K.; Fukuda, C.; Hori, K.; Sugimoto, H.; Nakanishi, E. *J. Polym. Sci., Part B: Polym. Phys.* **2007**, *45*, 129.

JA910901E